Chemokine-dependent T cell migration requires aquaporin-3–mediated hydrogen peroxide uptake

Mariko Hara-Chikuma,[1,2,4] Shunsuke Chikuma,[3] Yoshinori Sugiyama,[4] Kenji Kabashima,[1] Alan S. Verkman,[5,6] Shintaro Inoue,[4] and Yoshiki Miyachi[1]

[1]Department of Dermatology, [2]Center for Innovation in Immunoregulative Technology and Therapeutics, and [3]Department of Immunology and Genomic Medicine, Graduate School of Medicine, Kyoto University, Sakyo-ku, Kyoto 606-8501, Japan
[4]Innovative Beauty Science Laboratory, Kanebo Cosmetics Inc., Odawara, Kanagawa 250-0002, Japan
[5]Department of Medicine and [6]Department of Physiology, University of California, San Francisco, San Francisco, CA 94143

Chemokine-dependent trafficking is indispensable for the effector function of antigen-experienced T cells during immune responses. In this study, we report that the water/glycerol channel aquaporin-3 (AQP3) is expressed on T cells and regulates their trafficking in cutaneous immune reactions. T cell migration toward chemokines is dependent on AQP3-mediated hydrogen peroxide (H_2O_2) uptake but not the canonical water/glycerol transport. AQP3-mediated H_2O_2 transport is essential for the activation of the Rho family GTPase Cdc42 and the subsequent actin dynamics. Coincidentally, AQP3-deficient mice are defective in the development of hapten-induced contact hypersensitivity, which is attributed to the impaired trafficking of antigen-primed T cells to the hapten-challenged skin. We therefore suggest that AQP3-mediated H_2O_2 uptake is required for chemokine-dependent T cell migration in sufficient immune response.

CORRESPONDENCE
Mariko Hara-Chikuma:
haramari@kuhp.kyoto-u.ac.jp

Abbreviations used: AQP, aquaporin; CHS, contact hypersensitivity; DNFB, 2,4-dinitrofluorobenzene; DPI, diphenyleneiodonium; Nox, NADPH oxidase; Oxa, oxazolone; TNCB, 2, 4, 6-trinitro-1-chlorobenzene.

Regulated T cell migration and trafficking are of crucial importance for both steady-state T cell homeostasis and active immune responses. Although naive T cells constitutively circulate between the blood and secondary lymphoid organs in a state of immune surveillance, antigen-encountered T cells selectively migrate to extralymphoid sites to exert their secondary response to antigens (Mora and von Andrian, 2006; Pittet and Mempel, 2008). The mechanistic basis of regulated T cell trafficking involves the differential expression of adhesion molecules and chemokine receptors of naive and activated T cells (Campbell et al., 2003; Schaerli and Moser, 2005; Viola et al., 2006). The naive T cells express the LN homing receptor L-selectin (CD62L) and CCR7, enabling them to preferentially migrate to the secondary lymphoid organs (Campbell et al., 1998; Mora and von Andrian, 2006). In contrast, effector T cells express CCR4 and CCR10 instead of CD62L and CCR7, enabling them to migrate to peripheral nonlymphoid tissues, such as the gut and skin, in response to the chemokines CCL17, CCL22, and CCL27 (Campbell et al., 1999; Reiss et al., 2001). Such chemokine-dependent T cell migration requires actin-dependent changes in cell morphology and mobility, which are regulated by the Rho family GTPases, including Cdc42, Rac1, and RhoA (Burkhardt et al., 2008; Tybulewicz and Henderson, 2009).

Aquaporins (AQPs) are a family of highly conserved transmembrane channels that transport water and, in some cases, small solutes such as glycerol. Currently, 13 AQPs have been identified in mammals (AQP0–12). Numerous studies have demonstrated the fundamental importance of AQPs and have described their functions in several organs and physiological pathways, such as AQP1–3 in the urinary concentrating system, AQP1 in angiogenesis, AQP7 in obesity, and AQP4 in neuromyelitis optica and brain edema (Rojek et al., 2008; Verkman, 2009; Carbrey and Agre, 2009). More recently, some AQPs, including AQP3 and AQP8, have been found to mediate membrane

The Rockefeller University Press $30.00
J. Exp. Med. 2012 Vol. 209 No. 10 1743-1752
www.jem.org/cgi/doi/10.1084/jem.20112398

hydrogen peroxide (H_2O_2) uptake, which is used for intracellular signaling in mammalian cells (Miller et al., 2010). Despite their importance in various biological systems, to date, AQPs have not been shown to be involved in adaptive immunity, a process in which specialized lymphocytes at different developmental stages precisely mediate protection against pathogens to maintain homeostasis. Importantly, because previous studies have shown that AQPs regulate cell migration and proliferation in some mammalian cells (Verkman, 2009), we anticipated that AQPs might play a role in the regulation of lymphocyte function.

AQP3 is abundantly expressed on the plasma membrane of kidney-collecting duct principal cells and skin epidermal keratinocytes, which facilitate water and glycerol transport (Ma et al., 2000; Hara and Verkman, 2003). Our previous studies have shown that AQP3 is necessary for keratinocyte migration and proliferation, processes which have been implicated in cutaneous wound healing and tumorigenesis (Hara-Chikuma and Verkman, 2008a,b). During the course of our study, we unexpectedly found that the AQP3 protein was expressed not only by keratinocytes but also by skin-infiltrating T cells. In this study, using genetically modified AQP3 knockout mice, we have identified a novel role of AQP3 in chemokine-dependent T cell migration, which controls cutaneous immune reactions.

RESULTS

Normal cellularity and subpopulations of T cells in AQP3-null mice

Because we noted that AQP3 protein was expressed in skin-infiltrating T cells during contact hypersensitivity (CHS) in preliminary experiments, we focused on the function of AQP3 in T cells. Quantitative real-time RT-PCR analysis showed similar AQP3 expression levels in $CD4^+$ and $CD8^+$ cells; the expression levels were lower than those found in kidney extract, which is known to exhibit high AQP3 expression levels (Fig. 1 a; Ma et al., 2000). Using a germline AQP3 knockout ($AQP3^{-/-}$) mouse as a control (Ma et al., 2000), we verified the expression of AQP3 protein in both $CD4^+$ and $CD8^+$ T cells from WT mice using flow cytometry (Fig. 1 b).

To determine the function of AQP3 in T cells in vivo, phenotypic analysis was conducted on peripheral T cells and thymocytes from WT and $AQP3^{-/-}$ mice. $CD4^+$ and $CD8^+$ lymphocyte populations in the spleen, LNs, and thymus (Fig. 1, c and d), the expression of CD3, CD25, CD44, and CD62L in the thymus and LN (not depicted), and T cell proliferation levels (Fig. 1 e) from each of these preparations were similar between WT and $AQP3^{-/-}$ mice, indicating that the germline AQP3 deficiency did not affect T cell development or homeostasis under steady-state conditions.

Impaired chemotaxis efficiency and actin polymerization in AQP3-deficient T lymphocytes

Previous studies have demonstrated that AQP regulates the migration of several cell types (e.g., epithelial and endothelial cells), although the cellular and molecular mechanisms that underlie these processes remain controversial (Saadoun et al., 2005; Hara-Chikuma and Verkman, 2006, 2008a). We found that the efficiency of T cell migration toward several ligands (CXCL12, CCL19, CCL17, and CCL27) was significantly impaired in $AQP3^{-/-}$ T cells compared with WT T cells (Fig. 2 a), whereas no difference was found in T cell migration in the absence of chemokines (not depicted). Using chemotaxis chambers, WT T cells exhibited greater directed migration in response to CXCL12 chemotactic gradients than $AQP3^{-/-}$ T cells (Fig. 2 b). In response to CXCL12, transendothelial migration of $CD4^+$ T cells through vascular endothelial cells was also attenuated by AQP3 deficiency (Fig. 2 c). Conversely, cell adhesion was similar for both WT and $AQP3^{-/-}$ T cells (not depicted). In response to chemotactic signals, T cells reorganize their actin cytoskeletons and

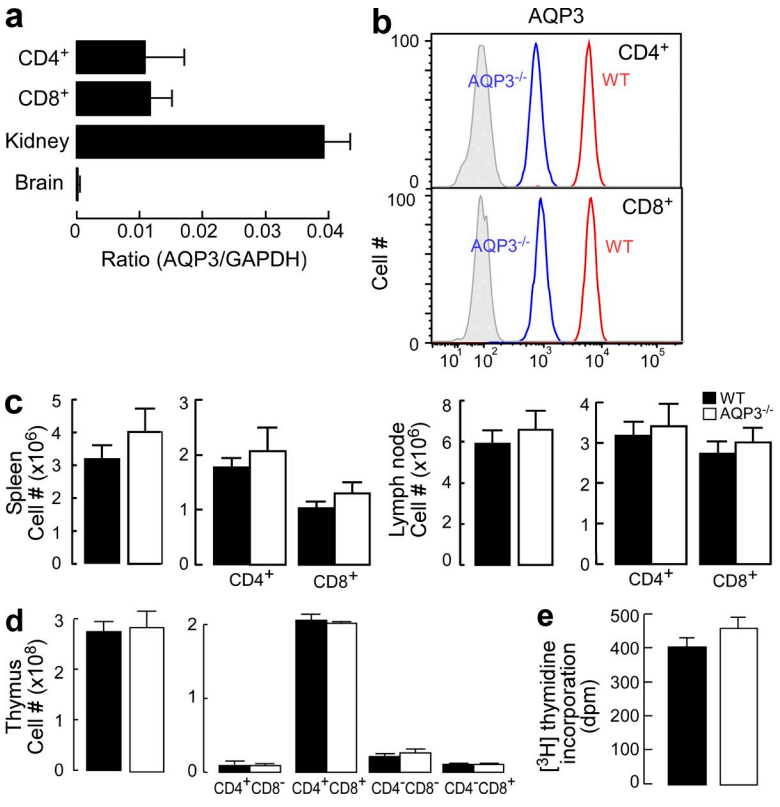

Figure 1. Normal cellularity and subpopulations of T cells in AQP3-null mice. (a) The messenger RNA expression levels of AQP3 in sorted $CD4^+$ and $CD8^+$ T cells as well as in kidney and brain tissues were assessed by real-time PCR (SE; $n = 4$). Data are expressed as the AQP3/GAPDH ratio. (b) Flow cytometric analysis of AQP3 expression in $CD4^+$ (top) or $CD8^+$ (bottom) T cells from WT and $AQP3^{-/-}$ mice. (c) Cell population analysis in the spleen (left) and LN (right). The numbers of total cells, $CD4^+$ and $CD8^+$ cells from WT and $AQP3^{-/-}$ mice (SE; $n = 4$), are shown. (d) Cell population analysis in the thymus. The numbers of total cells and indicated subsets (SE; $n = 4$) are shown. (e) [^{3}H]Thymidine incorporation in $CD4^+$ T cells from WT and $AQP3^{-/-}$ mice (SE; $n = 4$–5). Each experiment was performed three times.

become polarized in the direction of the chemoattractant gradient, which leads to chemotaxis and T cell trafficking (Burkhardt et al., 2008; Tybulewicz and Henderson, 2009). Chemokine-stimulated WT T cells developed a polarized morphology at the leading edge, which was visualized with phalloidin staining (Fig. 2 d, left). Immunofluorescence staining showed that AQP3 was localized at the leading edge as well as in the plasma membrane in CXCL12-treated T cells, whereas control T cells tended to express AQP3 both intracellularly and on the cell surface (Fig. 2 d, left). In contrast, AQP3$^{-/-}$ T cells failed to develop distinct uropods, instead exhibiting multiple, irregularly distributed areas of patch-like F-actin staining (Fig. 2 d, left). Chemokine-induced increase in the aspect ratio of a cell shape, which is defined as the length of the major axis divided by the width of the minor axis (Yang et al., 2005), was significantly impaired in AQP3$^{-/-}$ T cells compared with WT cells (Fig. 2 d, right). Consistent with these observations, quantification of F-actin levels revealed a significant impairment in chemokine-induced actin polymerization in AQP3$^{-/-}$ T cells in comparison with WT T cells (Fig. 2 e).

Impaired CHS with decreased T cell trafficking to challenged skin in AQP3-null mice

To determine the role of AQP3-mediated T cell trafficking in ongoing immune reactions, we used an experimental CHS model; specifically, we examined the T cell–mediated cutaneous immune/inflammatory reaction to haptens (Grabbe and Schwarz, 1998; Martin, 2004). WT and AQP3$^{-/-}$ mice were sensitized by applying haptens to the abdomen and were challenged on the ear 5 d later. Ear swelling (evidence of CHS) in response to the challenge with 2,4-dinitrofluorobenzene (DNFB), 2, 4, 6-trinitro-1-chlorobenzene (TNCB), and oxazolone (Oxa) was significantly decreased in AQP3$^{-/-}$ mice compared with WT mice (Fig. 3 a). Histological examination revealed pronounced spongiosis and extensive infiltration of lymphocytes in the dermis of WT mice, whereas such inflammation was mild in AQP3$^{-/-}$ mice (Fig. 3 a, right). A single application of DNFB or the nonspecific irritant croton oil induced identical ear swelling, indicating that non–T cell–mediated inflammatory responses were unaffected by AQP3 expression (not depicted).

AQP3 is expressed not only in T cells but also in epidermal keratinocytes, where it regulates cell proliferation (Hara-Chikuma and Verkman, 2008a,b). To exclude the possibility that the impaired CHS response in AQP3$^{-/-}$ mice was a result of compromised keratinocyte function, lethally irradiated C57BL/6 WT mice were

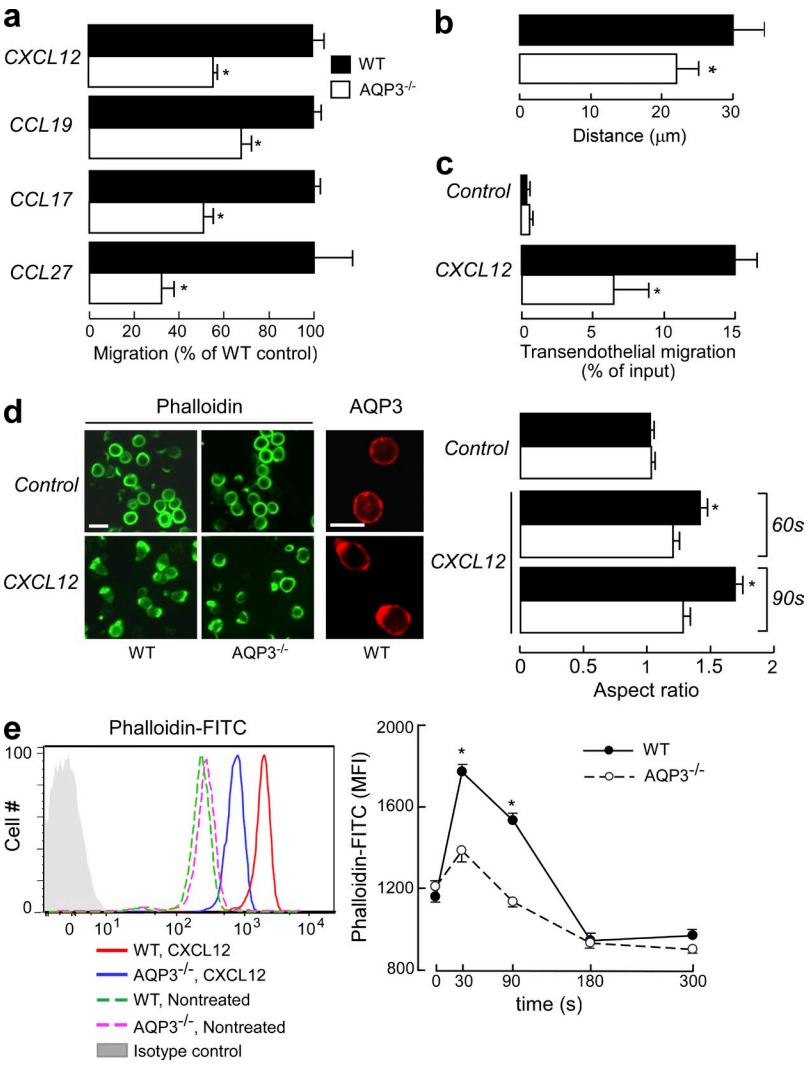

Figure 2. Impaired chemotaxis efficiency and F-actin polymerization levels of AQP3-deficient T lymphocytes. (a) Chemotaxis assay. The migration efficiency of CD4$^+$ T cells from WT and AQP3$^{-/-}$ mice toward the ligands CXCL12 (100 ng/ml), CCL19 (100 ng/ml), CCL17 (80 ng/ml), or CCL27 (80 ng/ml) was examined using a transwell chamber with 5-μm pores. Data are expressed as the percentage of WT control migration levels (SE; $n = 5$; *, $P < 0.01$). (b) Three-dimensional chemotaxis assay in response to CXCL12 gradient for 60 min. Accumulated distances for each cell (SE; $n = 50$; *, $P < 0.01$) are shown. (c) Transendothelial migration of CD4$^+$ T cells through mouse vascular endothelial cells (F-2 cells) in the presence of 100 ng/ml CXCL12 (SE; $n = 5$; *, $P < 0.01$). (d) CD4$^+$ WT and AQP3$^{-/-}$ T cells were stimulated with 500 ng/ml CXCL12 and stained with phalloidin-FITC (90 s) or with anti-AQP3 (3 min; cy3). (left) Representative immunofluorescence microscopy. Bars, 10 μm. (right) T cells were stimulated for 60 or 90 s with CXCL12. The aspect ratio of cell shape was quantified by measuring the length of the major axis divided by the width of the minor axis (SE; $n = 50$; *, $P < 0.01$). (e) T cells from WT and AQP3$^{-/-}$ mice were stimulated with 500 ng/ml CXCL12 and stained with phalloidin-FITC and CD4–Pacific blue. (left) Flow cytometry analysis of phalloidin-FITC gated on CD4$^+$ cells. One of four representative experiments is shown. (right) The mean fluorescence intensity (MFI) of phalloidin-FITC in the CD4$^+$ cells was analyzed (SE; $n = 5$; *, $P < 0.01$, WT vs. AQP3$^{-/-}$ cells). Each experiment was performed three times.

reconstituted with BM cells from either WT or AQP3$^{-/-}$ mice. Ear swelling was impaired in the chimeric mice reconstituted with AQP3-deficient BM cells compared with the response in mice reconstituted with WT BM cells (Fig. 3 b). These data indicate that the CHS response requires AQP3 expression on hematopoietic cells but not on keratinocytes.

We further examined the sensitization and elicitation phases of the CHS model. First, T cells from the draining LNs of WT and AQP3$^{-/-}$ mice were isolated 5 d after DNFB sensitization, and their responses to 2,4-dinitrobenzene sulfonic acid, a water-soluble compound with the same antigenicity as DNFB, were compared in vitro. We found comparable proliferative responses and IFN-γ production levels between WT and AQP3$^{-/-}$ mice (not depicted), suggesting that T cell priming occurred at equal levels in both groups of mice during the sensitization period.

Next, we investigated the elicitation phase of CHS using intravenous adoptive transfer. As shown in Fig. 3 c, the transfer of primed AQP3$^{-/-}$ T cells resulted in reduced ear swelling irrespective of AQP3 expression in the recipients compared with that resulting from the transfer of WT donor cells, suggesting that the cell-intrinsic defects in AQP3$^{-/-}$ T cells resulted in a defective elicitation of the immune response. To determine the involvement of AQP3 in T cell trafficking/homing during a secondary challenge in vivo, we adoptively transferred sensitized WT or AQP3$^{-/-}$ T cells that were labeled with a cell-tracking dye (CMFDA). Comparable numbers of CD4$^+$ CMFDA$^+$ T cells from WT and AQP3$^{-/-}$ mice were found in the LNs, whereas fewer skin-infiltrating T cells from AQP3$^{-/-}$ mice were observed than from WT mice (Fig. 3 d). The chemokine expression levels in the DNFB-challenged skin (not depicted), the chemokine receptor expression levels on the T cells (not depicted), and naive T cell homing into LNs (not depicted) were similar between WT and AQP3$^{-/-}$ mice.

Finally, we performed subcutaneous adoptive transfer experiments. When we injected sensitized LN cells directly into the ears of recipient WT or AQP3$^{-/-}$ mice, the AQP3$^{-/-}$ T cells overcame the defect and induced the same strong CHS that was observed with WT T cells (Fig. 3 e). Collectively, our findings provide evidence that AQP3 expression is important in the trafficking of T cells to antigen-challenged skin sites during CHS responses.

Impaired chemokine-induced Cdc42 activation in AQP3-deficient T lymphocytes

Our data suggest that AQP3 plays a fundamentally critical role in actin polymerization and subsequent T cell chemotaxis. The pathways that regulate actin dynamics are well characterized and involve Rho family small

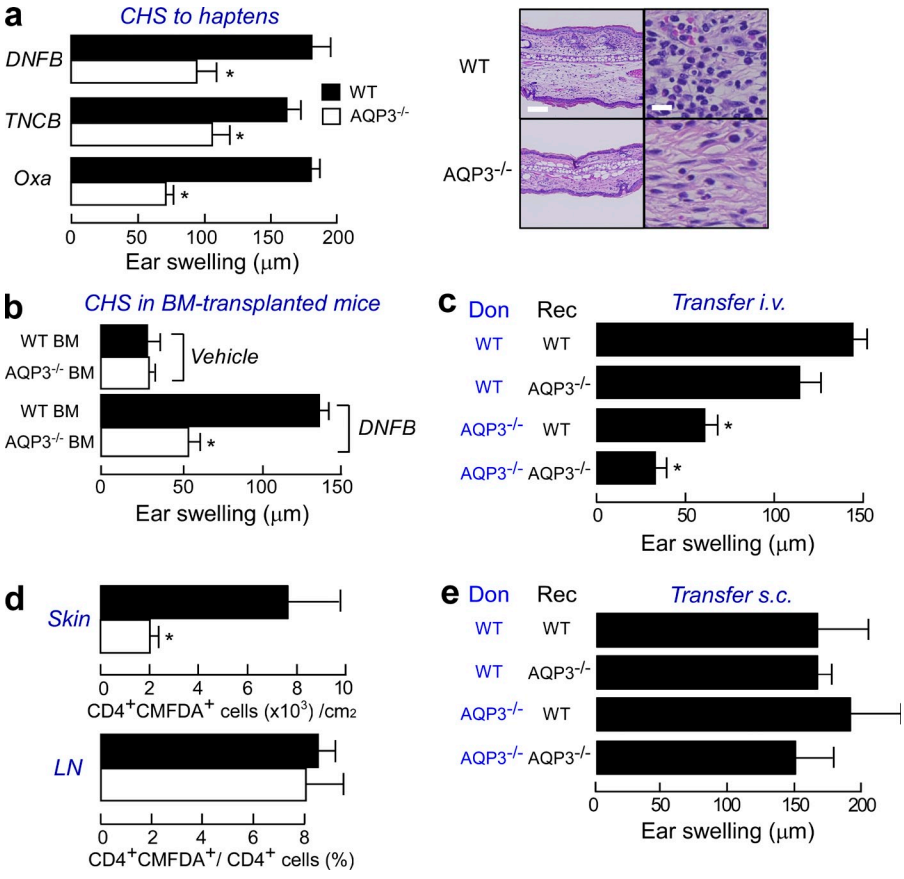

Figure 3. Impaired CHS with decreased T cell trafficking to a challenged skin site in AQP3-null mice. (a, left) Mice were sensitized with DNFB, TNCB, or Oxa and challenged 5 d later on the ear. The ear thickness was measured in micrometers 24 h after the challenge (SE; $n = 5$; *, $P < 0.01$). (right) Hematoxylin and eosin staining of the ears of sensitized WT and AQP3$^{-/-}$ mice at 24 h after challenge with DNFB. Bars: (left) 100 μm; (right) 20 μm. (b) CHS test using BM cell–transferred mice. C57BL/6 mice received transplants of BM cells from WT and AQP3$^{-/-}$ mice. The CHS test was performed with DNFB 2 mo later (SE; $n = 4$; *, $P < 0.01$). (c) Adoptive transfer experiments by intravenous injection. LN cells from sensitized donor WT and AQP3$^{-/-}$ mice (Don) were injected intravenously (3×10^7 cells/head) to recipient mice (Rec). Ear swelling at 24 h after challenge (SE; $n = 3$–5; *, $P < 0.01$) is shown. (d) Adoptive transfer experiments by intravenous injection. LN cells from sensitized WT and AQP3$^{-/-}$ donors were stained with CMFDA and injected into recipient WT mice, and these mice were challenged with 0.3% DNFB. The ear skin, which was painted with DNFB, and LNs were excised 24 h after challenge. CD4$^+$ and CMDFA$^+$ cells were analyzed by flow cytometric analysis (SE; $n = 4$; *, $P < 0.01$). (e) Adoptive transfer experiments by subcutaneous injection (2×10^5 cells) into the ears. Ear swelling at 24 h after challenge is shown (SE; $n = 4$). Experiments in a, c, and e were performed in two other independent experiments and in b and d in one other experiment with similar results.

GTPases such as Cdc42, Rac1, and RhoA. To gain insight into the molecular mechanism that regulates AQP3-mediated actin polymerization, we examined the activation of each GTPase upon CXCL12 stimulation. Quantification of the activated forms of each GTPase using a colorimetry-based assay revealed a complete impairment in Cdc42 activation in response to CXCL12 in AQP3$^{-/-}$ T cells (Fig. 4 a). Compared with WT cells, AQP3$^{-/-}$ cells exhibited minimal activation of Rac1, although this difference was not statistically significant (Fig. 4 b). CXCL12-induced Rac1 activation was lower in AQP3$^{-/-}$ than in WT T cells ($P < 0.07$). We considered that Rac1 activation was also attenuated by AQP3 deficiency. No difference was found between AQP3$^{-/-}$ and WT cells for CXCL12-induced RhoA activation (Fig. 4 c).

Cdc42 activates WASP (Wiskott-Aldrich syndrome protein), which, through the Arp2/3 protein complex, leads to actin polymerization (Burkhardt et al., 2008; Tybulewicz and Henderson, 2009). AQP3$^{-/-}$ T cells also exhibited a defect in CXCL12-induced phosphorylation of WASP and Arp2 (Fig. 4 d). Moreover, Tec family tyrosine kinase Itk has been suggested to be one of the upstream signaling molecules of CXCL12-induced Cdc42 and Rac1 activation pathways (Fischer et al., 2004; Takesono et al., 2004). Fig. 4 e showed the impairment of CXCL12-induced Itk phosphorylation in AQP3$^{-/-}$ T cells.

We next sought to examine the implications of AQP3-mediated Cdc42 activation in terms of actin polymerization using dominant-active (V12-Cdc42) mutants of Cdc42. Given the technical difficulty of transfecting primary mouse T cells, we established an experimental protocol in which endogenous AQP3 was efficiently knocked down by siRNA and subsequently transfected with exogenous Cdc42-cDNA in human T cells. AQP3 knockdown in human T cells reproduced the impaired chemokine-induced actin polymerization (Fig. 4 f) and chemotaxis (not depicted) observed in AQP3$^{-/-}$ mouse T cells. In this setting, impaired actin polymerization was restored by the expression of V12-Cdc42 (Fig. 4 g). These findings suggest that AQP3 is required for chemokine-induced actin polymerization and polarization of T cells through the activation of pathways involving Cdc42.

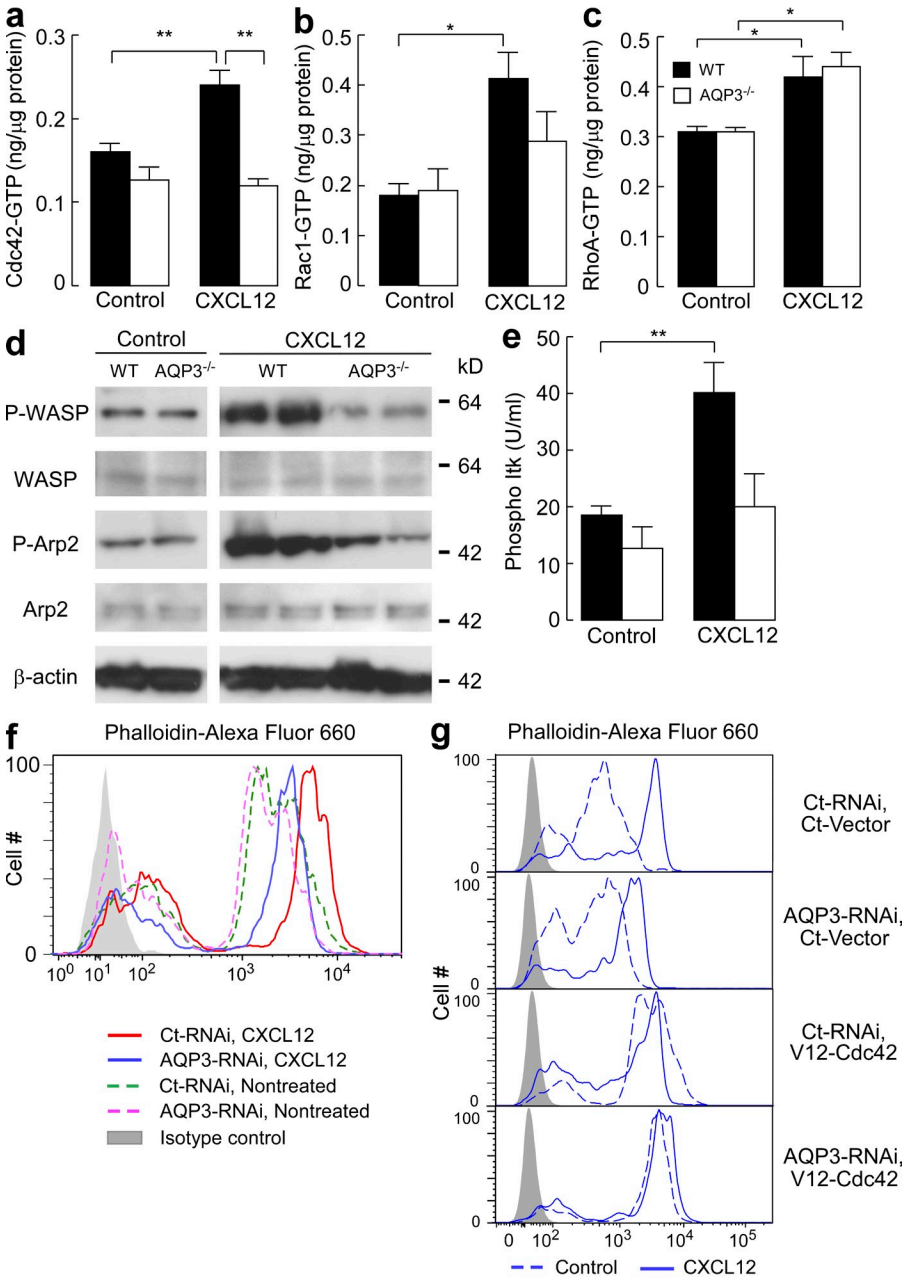

Figure 4. Impaired chemokine-induced Cdc42 activation in AQP3-deficient T cells. (a–c) Quantifications of Cdc42, Rac1, and RhoA activation. T cells were incubated with 250 ng/ml CXCL12 for 1 min, and GTP-bound active form of Cdc42 (a), Rac1 (b), and RhoA (c) were assessed using the G-LISA activation assay kit (SE; $n = 4–5$; *, $P < 0.05$; **, $P < 0.01$). (d) Immunoblot analyses to detect the phosphorylation of WASP and Arp2. T cells were incubated with 250 ng/ml CXCL12 for 3 min and were analyzed using antibodies against phospho-WASP (P-WASP), WASP, phospho-Arp2, Arp2, and β-actin. The blots shown are representative of three separate sets of experiments. (e) Phosphorylated Itk in response to CXCL12 (250 ng/ml, 1 min) was quantified with BD cytometric bead array (SE; $n = 4–5$; **, $P < 0.01$). (f and g) F-actin polymerization in response to 500 ng/ml CXCL12 in AQP3 knockdown (f) and/or V12-Cdc42–positive human primary T cells (g). One representative experiment of three experiments is shown. Experiments in a–c and e were performed in two other independent experiments.

Water/H_2O_2 permeability is dependent on AQP3 expression in T cells

To further investigate the mechanism underlying AQP3-mediated T cell chemotaxis, we examined whether the membrane transport of water, glycerol, and H_2O_2, which may affect cellular activities, occurred in T cells in an AQP3-dependent manner. The osmotic water permeability of $CD4^+$ T cells was measured using the kinetics of scattered light intensity in response to osmotic challenge (Fig. 5 a, left), as previously described (Yang et al., 2001). Water transport in response to a 150-mM inwardly directed mannitol gradient was significantly higher in WT than in $AQP3^{-/-}$ T cells (Fig. 5 a, right). In contrast, no difference was found in the glycerol transport levels between the WT and $AQP3^{-/-}$ T cells (Fig. 5 b). In T cells, glycerol permeability might be facilitated primarily by diffusion through the membrane or other AQPs because the permeability levels were much higher than those observed in other cells such as erythrocytes (Yang et al., 2001). We measured intracellular H_2O_2 levels using CM-H2DCFDA fluorescence and identified reduced cellular H_2O_2 levels in $AQP3^{-/-}$ $CD4^+$ T cells (Fig. 5 c). Exogenous H_2O_2 supplementation for 15 s increased cellular H_2O_2 levels to a significantly greater extent in WT than in $AQP3^{-/-}$ $CD4^+$ T cells, suggesting the involvement of AQP3 in H_2O_2 transport in T cells (Fig. 5 c).

We next investigated the effects of a chemokine on cellular H_2O_2 concentration and its production in T cells. As shown in Fig. 5 d, CXCL12 stimulation markedly increased intracellular H_2O_2 levels in WT $CD4^+$ T cells within 15 s. Previous studies have reported that T cells generate H_2O_2 via NADPH oxidase (Nox), which was considered to regulate TCR signaling or adaptive immune responses (Jackson et al., 2004; Purushothaman and Sarin, 2009). Pretreatment with diphenyleneiodonium (DPI), a general Nox inhibitor, or incubation with catalase, which removes any extracellular H_2O_2, significantly suppressed CXCL12-induced intracellular H_2O_2 levels in WT cells (Fig. 5 d). This suggested that CXCL12 stimulation activates Nox for the extracellular production of H_2O_2. $AQP3^{-/-}$ $CD4^+$ T cells also showed a significant increase in cellular H_2O_2 levels at 15–30 s after CXCL12 stimulation, although this increase was minimal as compared with that in WT cells (Fig. 5 e). Collectively, our results suggest that CXCL12 stimulation increases the intracellular H_2O_2 level, which was dependent on AQP3 in T cells.

AQP3-mediated H_2O_2 transport is required for CXCL12-induced Cdc42 activation and chemotaxis

Recent evidence has suggested a role of cellular H_2O_2 as a signaling intermediate in the regulation of a variety of biological processes, including growth, differentiation, and migration

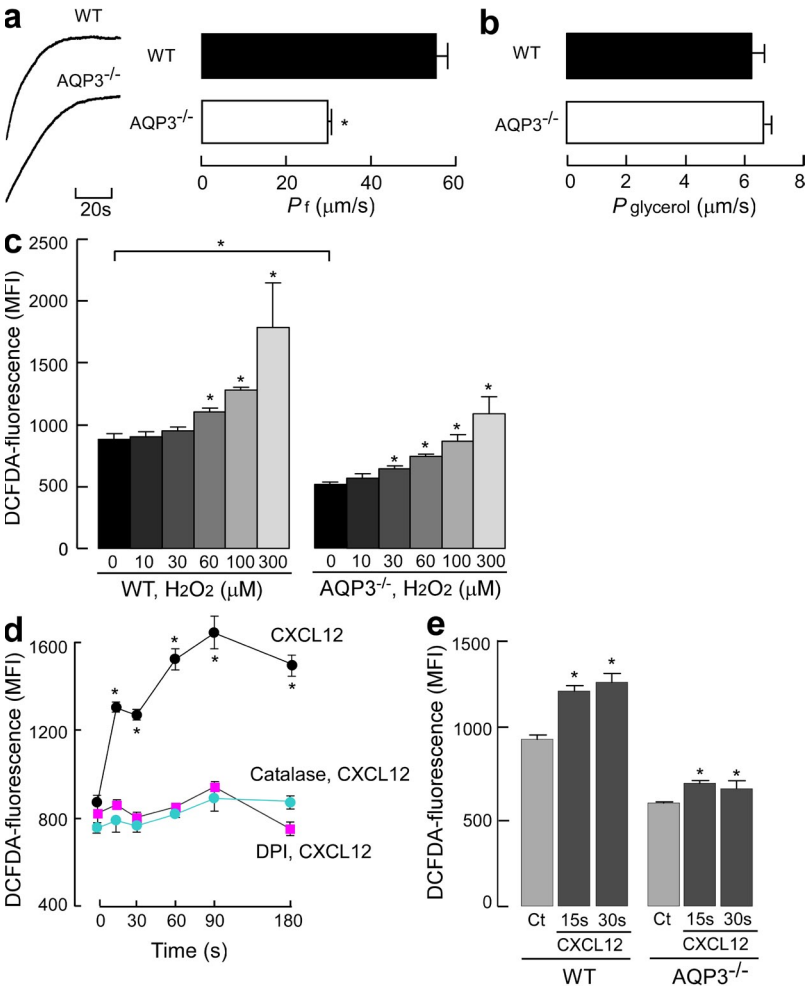

Figure 5. Water and H_2O_2 permeability depended on AQP3 expression in T cells. (a) The osmotic water permeability of $CD4^+$ T cells isolated from WT and $AQP3^{-/-}$ mice was measured based on the time course of scattered light intensity in response to a 150-mM inwardly directed mannitol gradient generated by stopped flow at 22°C. (left) Representative time course data showing responses to rapid changes in perfusate osmolality between 300 and 450 mOsm. (right) Averaged osmotic water permeability coefficients (P_f; SE; $n = 5$; *, $P < 0.01$). (b) Glycerol permeability was measured in response to a 150-mM inwardly glycerol gradient by stopped flow at 30°C (SE; $n = 4$). (c) H_2O_2 uptake into T cells. $CD4^+$ T cells were incubated with 10–300 μM H_2O_2 for 15 s, and cellular H_2O_2 levels were detected using CM-H2DCFDA reagent by flow cytometric analysis. The mean fluorescence intensity (MFI) of CM-H2DCFDA fluorescence (SE; $n = 4$; *, $P < 0.01$, H_2O_2 added vs. control cells) is shown. (d) WT $CD4^+$ cells were incubated with 5 μM DPI or 2,000 U/ml catalase for 30 min and followed with 500 ng/ml CXCL12 for 15–180 s at 37°C. $CD4^+$ cellular H_2O_2 levels were detected using CM-H2DCFDA reagent by flow cytometry analysis (SE; $n = 5$; *, $P < 0.01$, CXCL12 treated vs. control cells). (e) Cellular H_2O_2 levels in WT and $AQP3^{-/-}$ $CD4^+$ cells after CXCL12 stimulation (500 ng/ml, 15 or 30 s; SE; $n = 5$; *, $P < 0.01$ vs. control cells). Each experiment was performed three times.

(Stone and Yang, 2006; Veal et al., 2007; Poole and Nelson, 2008; Paulsen and Carroll, 2010). We first sought to determine whether intracellular H_2O_2 is involved in CXCL12-induced downstream cellular signaling. Treatment with catalase or DPI suppressed CXCL12-induced Cdc42 activation and Itk phosphorylation (Fig. 6, a and b). CXCL12-mediated actin polymerization was also prevented by treatment with catalase or DPI (Fig. 6 c). Furthermore, treatment of WT T cells with catalase or DPI attenuated the chemotactic efficacy in response to CXCL12 (Fig. 6 d).

Next, we determined whether the exogenous addition of H_2O_2 could modulate Itk and Cdc42 activation. Fig. 6 (e and f) shows that an exogenously added high dose of H_2O_2 (100 μM) induced Itk phosphorylation and Cdc42 activation in WT T cells, whereas no activation was found in AQP3$^{-/-}$ T cells (not depicted). These results confirmed the involvement of intracellular H_2O_2 in CXCL12-induced cell signaling for chemotaxis in T cells.

Having observed the robust uptake of extracellular H_2O_2 through AQP3 in T cells, we next examined the significance of AQP3-mediated H_2O_2 uptake in CXCL12-induced cell signaling and T cell chemotaxis. As shown in Fig. 5 c, when AQP3$^{-/-}$ T cells were exogenously supplemented with 100 μM H_2O_2 for 15 s, the intracellular concentration of H_2O_2 was equivalent to that observed in control WT T cells in which H_2O_2 might be transported through other AQPs or may diffuse across the plasma membrane. CXCL12 stimulation together with exogenous addition of 100 μM H_2O_2 for 15 s remarkably increased the level of DCFDA in AQP3$^{-/-}$ T cells. This was equal to that observed in WT T cells with 100-μM-H_2O_2 supplementation or CXCL12 stimulation (Fig. 7 a). In this context, as shown in Fig. 7 (b and c), AQP3$^{-/-}$ T cells exhibited significant improvements in CXCL12-induced Itk phosphorylation and Cdc42 activation. Furthermore, impaired F-actin polymerization in response to CXCL12 observed in AQP3$^{-/-}$ T cells was recovered by adding exogenous 100 μM H_2O_2 and CXCL12 stimulation (Fig. 7 d). Finally, we found that pretreating AQP3$^{-/-}$ T cells with 100 μM H_2O_2 improved decreased chemotaxis in response to CXCL12 resulting from AQP3 deficiency (Fig. 7 e). These results provide evidence that AQP3-mediated H_2O_2 transport plays an important role in T cell chemotaxis.

DISCUSSION

Our current data reveal a previously unrecognized role of AQP3 in T cell–mediated immunity. First, AQP3 deficiency impaired the water/H_2O_2 permeability and migration of T cells, which was accompanied by defective F-actin dynamics and Cdc42 activation in response to chemokines. Second, AQP3$^{-/-}$ mice showed a severe resistance to CHS development. A direct injection of primed AQP3$^{-/-}$ T cells to the site of the secondary challenge completely reconstituted CHS, suggesting that this defect was based solely on the trafficking of T cells to regional sites. Third, the attenuation of the intracellular H_2O_2 level suppressed chemokine-induced Cdc42 activation, F-actin dynamics, and cell migration. Last, exogenous supplementation with H_2O_2, which restored the reduced cellular H_2O_2 levels in AQP3$^{-/-}$ T cells to the levels observed in WT T cells (presumably by passive diffusion), rescued all the defects in AQP3-deficient T cells, including chemokine-induced Cdc42 activation, actin dynamics, and chemotaxis. Collectively, these findings suggest that AQP3-mediated H_2O_2 transport is required for Cdc42 activation and chemokine-dependent T cell migration, which regulates T cell trafficking during CHS.

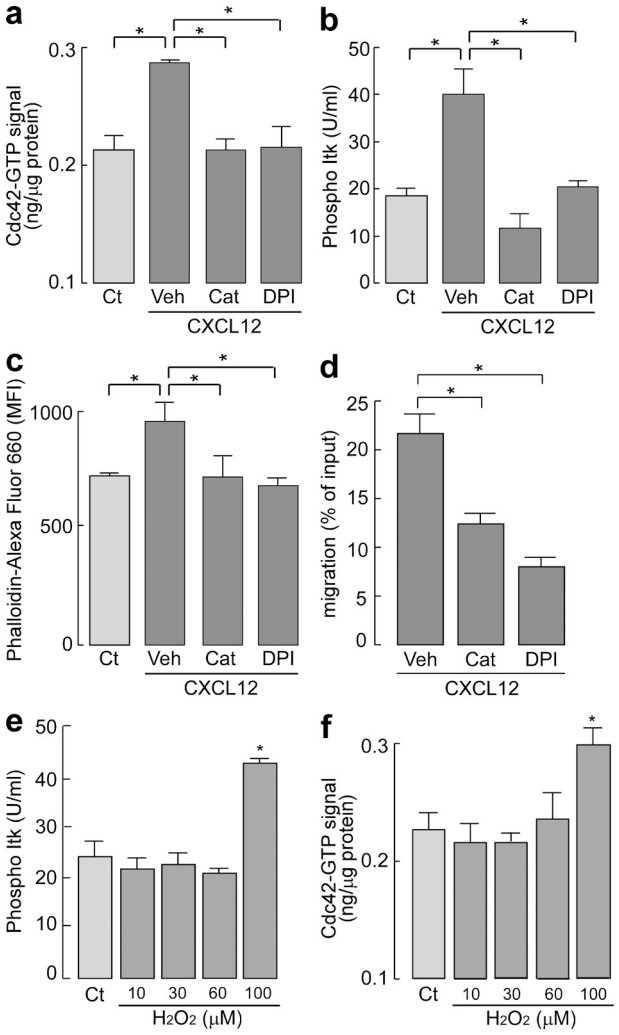

Figure 6. Intracellular H_2O_2 affects CXCL12-induced cell signaling and chemotaxis. (a–c) CD4$^+$ T cells were incubated with 2,000 U/ml catalase (Cat), 5 μM DPI, or vehicle (Veh) for 30 min at 37°C and stimulated with 250 or 500 ng/ml CXCL12. (a) Quantification of Cdc42 active form (GTP bound) with G-LISA activation assay kit (SE; $n = 4–5$; *, $P < 0.01$). (b) Cytometric bead array–based quantification of phosphorylated Itk (SE; $n = 4–5$; *, $P < 0.01$). (c) Mean fluorescence intensity (MFI) of phalloidin–Alexa Fluor 660 in the CD4$^+$ cells (SE; $n = 5$; *, $P < 0.01$). (d) Chemotaxis assay toward 100 ng/ml CXCL12 for 1 h (SE; $n = 5$; *, $P < 0.01$). (e and f) CD4$^+$ T cells were incubated with 10–100 μM H_2O_2 for 1 min at 37°C. (e) Quantification of Cdc42 active form (GTP bound; SE; $n = 4$; *, $P < 0.01$). (f) The amount of phosphorylated Itk (SE; $n = 4$; *, $P < 0.01$). Experiments in a–d were performed in two other independent experiments and in e and f in one other experiment with similar results.

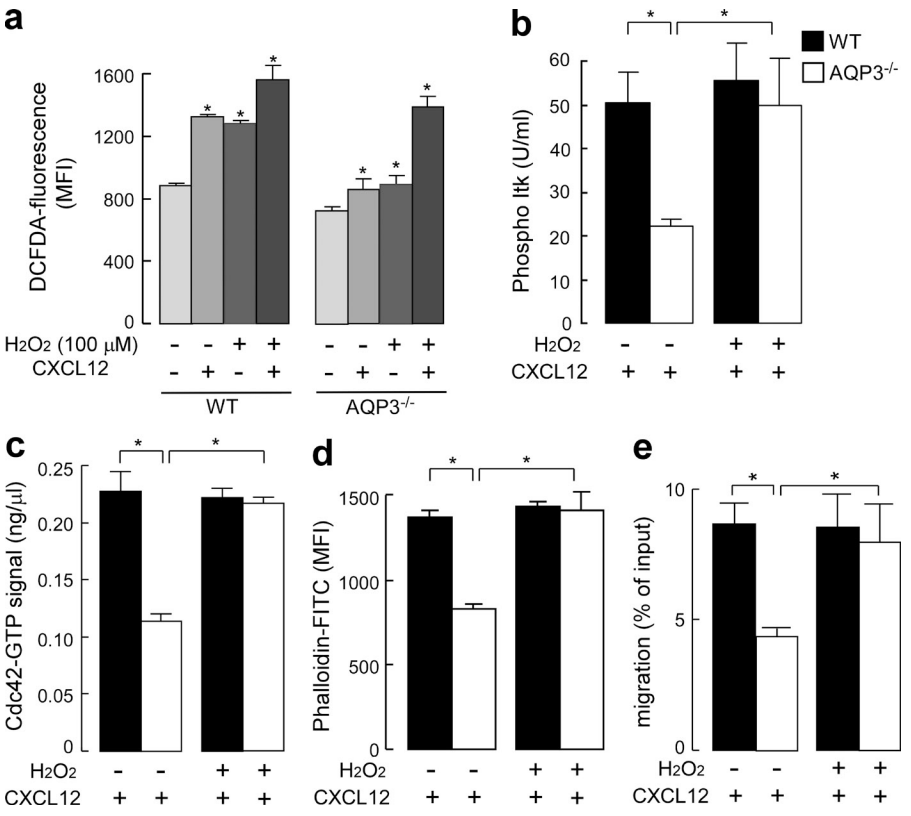

Figure 7. H_2O_2 supplementation restored the impaired cell signaling and chemotaxis in AQP3-deficient T cells. (a–d) CD4+ T cells from WT and AQP3$^{-/-}$ mice were stimulated by 500 ng/ml CXCL12 together with/without exogenous addition of 100 μM H_2O_2. (a) Intracellular H_2O_2 levels for 15 s (SE; $n = 4$; *, $P < 0.01$, treated vs. control cells). (b) The amount of phosphorylated Itk (SE; $n = 4$; *, $P < 0.01$). (c) Quantification of Cdc42 active form (GTP bound; SE; $n = 4$; *, $P < 0.01$). (d) Mean fluorescence intensity (MFI) of phalloidin-FITC in the CD4+ cells was analyzed (SE; $n = 4$; *, $P < 0.01$). (e) T cells were incubated with 100 μM H_2O_2 for 15 s, washed, and assayed for chemotaxis for 30 min toward 200 ng/ml CXCL12 (SE; $n = 5$; *, $P < 0.01$). Experiments were performed in one other experiment with similar results.

In earlier studies (Schröder and Eaton, 2008), H_2O_2 was appreciated only as a marker for oxidative stress, and it was shown to be associated with various pathological conditions such as angiogenesis, cancer, and aging. Recent evidence revealed that H_2O_2 is not only important for such pathologies, but also plays an essential role in cellular physiology as a signaling molecule (Rhee, 2006; Stone and Yang, 2006; Veal et al., 2007; Schröder and Eaton, 2008; Yoo et al., 2011). In the past, extracellular H_2O_2 was thought to passively diffuse across the plasma membrane. Recently, however, yeast and plants were reported to actively transport H_2O_2 through membrane AQPs such as TIP1 (Bienert et al., 2007; Ludewig and Dynowski, 2009). Moreover, mammalian AQP3 was shown to mediate the uptake of H_2O_2 (Miller et al., 2010). In this study, we found that AQP3 transports H_2O_2 and regulates the intracellular H_2O_2 level in T cells, which is essential for chemokine-induced cell signaling, at least in terms of the activation of Cdc42. The precise mechanism by which AQP3-mediated H_2O_2 is involved in CXCL12-induced Cdc42 activation remains unknown. Although the protein tyrosine phosphatase family has been recognized as one of the potential targets of H_2O_2 in cell signaling, other molecular targets of H_2O_2 or H_2O_2-based signal transduction are still largely unknown (Rhee, 2006; Poole and Nelson, 2008; Paulsen and Carroll, 2010). The membrane activation of the Tec family kinase Itk in T cells is believed to require CXCL12-induced activation of Cdc42 and Rac1 (Fischer et al., 2004; Takesono et al., 2004). Indeed, we found not only the defect of Cdc42 activation and the attenuation of Rac1 activation, but also a loss of Itk phosphorylation in response to CXCL12 in AQP3$^{-/-}$ T cells. In addition, our data suggests that CXCL12 stimulation induces a substantial amount of H_2O_2 production, probably because of the activation of Nox, which is transported inward by AQP3 in T cells. AQP3 immunostaining suggested that upon CXCL12 stimulation, AQP3 may be translocated to the leading edge of a cell membrane where it could facilitate H_2O_2 transport. Although further studies are required to elucidate the mechanism underlying the involvement of AQP3-mediated H_2O_2 transport in cell signaling pathways, we hypothesize that AQP3-facilitated intracellular H_2O_2 is involved in chemokine-induced Itk and Cdc42/Rac1 activation and subsequently regulates the downstream protein WASP and the Arp2/3 protein complex. Together, these play a key role in the formation of filopodia and lamellipodia during T cell trafficking.

We propose that AQP3, in addition to its known biological importance, should be considered a target for T cell–mediated diseases. For example, inflammatory skin diseases, such as atopic dermatitis and psoriasis, are characterized by the infiltration of T cells into both the dermis and the epidermis of affected skin, whereas different subsets of T cells are associated with each disease (Guttman-Yassky et al., 2011). In our study, we found abundant T cell infiltrates with AQP3 expression in the skin of the atopic dermatitis and psoriatic lesions (unpublished data), suggesting that these pathologies also involve AQP3-mediated T cell migration to the skin. Future studies may provide novel therapeutic strategy for controlling unwanted immune reactions in the skin, including atopic dermatitis and psoriasis, and other autoimmune diseases.

MATERIALS AND METHODS

Mice. AQP3$^{-/-}$ mice (C57BL/6 genetic background) were generated by targeted gene disruption (Ma et al., 2000). All comparisons were between

littermates. All animal experiments were approved by the Committee on Animal Research of Kyoto University.

Flow cytometry analysis. Single cell suspensions were stained with monoclonal antibodies against CD3, CD4, CD8, CD25, CD44, or CD62L (eBioscience). To assess their cellular F-actin content, we fixed lymphocytes in 4% formalin in PBS, permeabilized with 0.1% Triton X-100, and stained with Alexa Fluor 488– or Alexa Fluor 660–conjugated phalloidin (Invitrogen). The samples were analyzed using the flow cytometry FACSCanto II system (BD).

Immunohistochemistry and immunofluorescence microscopy. Paraffin-embedded sections were stained with hematoxylin and eosin. For cell polarization, cells were cultured on poly-lysine–coated coverslips and stimulated with CXCL12. Cells were fixed with 4% formalin in PBS, permeabilized with 0.1% saponin, and stained with Alexa Fluor 488–phalloidin or anti-AQP3 (Millipore).

Immunoblotting, GTPase assays, and Itk assay. To analyze chemokine-induced protein phosphorylation, cells were lysed with ice-cold lysis buffer (Cell Signaling Technology). The supernatant (14,000 *g*, 10 min, 4°C) was used for immunoblotting with antibodies against phospho-Arp2, phospho-WASP (ECM Biosciences), Arp2 (Millipore), WASP (Santa Cruz Biotechnology, Inc.), and β-actin (Sigma-Aldrich). The activation of Rho family small GTPases was detected using G-LISA Rho, Rac1, or Cdc42 activation Biochem kit (Cytoskeleton) according to the manufacturer's instructions. The amount of phospho Itk was assayed with Itk BD cytometric bead array (BD) according to the manufacturer's instructions.

Water, glycerol, and H_2O_2 permeability assay. Water and glycerol permeability were measured using an SX20 stopped-flow spectrometer (Applied Photophysics). The sorted T cells in RPMI medium were subjected to a 150-mM inwardly directed Mannitol or glycerol gradient. The kinetics of the decreasing cell volumes was measured from the time course of 90° scattered light intensity at 450 nm wavelength. Osmotic water/glycerol permeability coefficients (P_f) were calculated as described previously (Yang et al., 2001). Cellular H_2O_2 was assayed using the CM-H2DCFDA reagent (Invitrogen) according to the manufacturer's instructions.

Chemotaxis and transendothelial migration assays. T cells from the LNs of WT and AQP3$^{-/-}$ mice (10^6 cells) were deposited on the upper chamber containing a polycarbonate transwell membrane filter (5-µm pore size; Corning). The lower chamber contained 100 ng/ml CXCL12, 100 ng/ml CCL19, 80 ng/ml CCL17, or 80 ng/ml CCL27 in RPMI complete medium. The recovered cells were analyzed with flow cytometry analysis.

Three-dimensional chemotaxis assay was performed using the µ-Slide chemotaxis chamber (Ibidi) according to the manufacturer's instructions. WT or AQP3$^{-/-}$ T cells in collagen gel (3×10^6 cell/ml) were applied to the chamber. Cell movement in response to CXCL12 gradient was tracked for 60 min and analyzed using National Institutes of Health ImageJ.

For transendothelial migration, mouse vascular endothelial cell line (F-2; Toda et al., 1990) was seeded onto a 5-µm transwell filter and grown to confluence. T cells (10^6 cells) were deposited on the upper chamber, and RPMI complete medium containing 100 ng/ml CXCL12 was added to the lower chamber. After 8 h, the transmigrated cells were counted by flow cytometry analysis.

RNAi and plasmid DNAs. To knock down the AQP3 gene, human T cells were incubated with Accell AQP3 siRNA or Accell Non-Targeting siRNA in Accell siRNA delivery medium (Thermo Fisher Scientific) for 48–72 h. AQP3 expression was confirmed by flow cytometry analysis and quantitative PCR. The cDNA from plasmid for dominant-active mutants of Cdc42 (V12-Cdc42; a gift from S. Narumiya, Kyoto University, Sakyo-ku, Kyoto, Japan) was transfected with TransIT (Takara Bio Inc.).

CHS. Mice were sensitized with 50 µl of 0.5% DNFB, 5% TNCB, or 5% Oxa solution on the abdomen. 5 d later, 20 µl of each hapten was applied to the left ear, and the vehicle (acetone/olive oil, 4:1) was applied to the right ear. Ear swelling was measured with a spring-loaded micrometer (Mitutoyo) 24 h after challenge.

Adoptive transfer experiments. Cell suspensions obtained from the LNs of DNFB-sensitized mice were injected subcutaneously (2×10^5 per 20 µl PBS) or intravenously (3×10^7 cells/head) into the ears of naive WT and AQP3$^{-/-}$ mice. The ears were immediately challenged by applying 20 µl of 0.3% DNFB or vehicle to both sides of the ear. Ear thickness was measured after 24 h. To track the transferred cells, the isolated cells derived from DNFB-sensitized mice were stained with CMFDA for 20 min, washed, and injected intravenously (4×10^7 cells/head). The ear and regional LN were excised at 24 h after DNFB application, and the cells were isolated with collagenase and trypsin treatment. CD4$^+$ and CMFDA$^+$ cells were analyzed by flow cytometry analysis.

BM transplantation. BM cells from WT and AQP3$^{-/-}$ mice were subjected to hypotonic red blood cell lysis. C57BL/6 recipients (8–10 wk old) were γ irradiated with two doses of 600 rad (3 h apart). After irradiation, the mice received 10^6 BM cells intravenously. This protocol constantly gave >90% reconstitution of the recipient by donor hematopoietic cells, as evaluated by a separate transplantation experiment using BM from C57BL/6-CD45.1 congenic mice. The CHS test was performed 2 mo later.

Statistical analysis. Statistical analysis was performed using the two-tailed Student's *t* test or analysis of variance.

We thank Kiiko Kumagai and Kayo Nishida for mouse breeding, Dr. Yoshinori Fujiyoshi and Akiko Kamegawa for help with water transport measurement, and Dr. Shuh Narumiya for critical reading of the manuscript.

This work was supported in part by grants from the Ministry of Education, Culture, Sports, Science and Technology of Japan.

The authors declare no financial conflicts of interest.

Submitted: 11 November 2011
Accepted: 3 August 2012

REFERENCES

Bienert, G.P., A.L. Møller, K.A. Kristiansen, A. Schulz, I.M. Møller, J.K. Schjoerring, and T.P. Jahn. 2007. Specific aquaporins facilitate the diffusion of hydrogen peroxide across membranes. *J. Biol. Chem.* 282:1183–1192. http://dx.doi.org/10.1074/jbc.M603761200

Burkhardt, J.K., E. Carrizosa, and M.H. Shaffer. 2008. The actin cytoskeleton in T cell activation. *Annu. Rev. Immunol.* 26:233–259. http://dx.doi.org/10.1146/annurev.immunol.26.021607.090347

Campbell, D.J., C.H. Kim, and E.C. Butcher. 2003. Chemokines in the systemic organization of immunity. *Immunol. Rev.* 195:58–71. http://dx.doi.org/10.1034/j.1600-065X.2003.00067.x

Campbell, J.J., E.P. Bowman, K. Murphy, K.R. Youngman, M.A. Siani, D.A. Thompson, L. Wu, A. Zlotnik, and E.C. Butcher. 1998. 6-C-kine (SLC), a lymphocyte adhesion-triggering chemokine expressed by high endothelium, is an agonist for the MIP-3β receptor CCR7. *J. Cell Biol.* 141:1053–1059. http://dx.doi.org/10.1083/jcb.141.4.1053

Campbell, J.J., G. Haraldsen, J. Pan, J. Rottman, S. Qin, P. Ponath, D.P. Andrew, R. Warnke, N. Ruffing, N. Kassam, et al. 1999. The chemokine receptor CCR4 in vascular recognition by cutaneous but not intestinal memory T cells. *Nature.* 400:776–780. http://dx.doi.org/10.1038/23495

Carbrey, J.M., and P. Agre. 2009. Discovery of the aquaporins and development of the field. *Handb Exp Pharmacol.* 190:3–28. http://dx.doi.org/10.1007/978-3-540-79885-9_1

Fischer, A.M., J.C. Mercer, A. Iyer, M.J. Ragin, and A. August. 2004. Regulation of CXC chemokine receptor 4-mediated migration by the Tec family tyrosine kinase ITK. *J. Biol. Chem.* 279:29816–29820. http://dx.doi.org/10.1074/jbc.M312848200

Grabbe, S., and T. Schwarz. 1998. Immunoregulatory mechanisms involved in elicitation of allergic contact hypersensitivity. *Immunol. Today.* 19:37–44. http://dx.doi.org/10.1016/S0167-5699(97)01186-9

Guttman-Yassky, E., K.E. Nograles, and J.G. Krueger. 2011. Contrasting pathogenesis of atopic dermatitis and psoriasis—part I: clinical and pathologic concepts. *J. Allergy Clin. Immunol.* 127:1110–1118. http://dx.doi.org/10.1016/j.jaci.2011.01.053

Hara, M., and A.S. Verkman. 2003. Glycerol replacement corrects defective skin hydration, elasticity, and barrier function in aquaporin-3-deficient mice. *Proc. Natl. Acad. Sci. USA.* 100:7360–7365. http://dx.doi.org/10.1073/pnas.1230416100

Hara-Chikuma, M., and A.S. Verkman. 2006. Aquaporin-1 facilitates epithelial cell migration in kidney proximal tubule. *J. Am. Soc. Nephrol.* 17:39–45. http://dx.doi.org/10.1681/ASN.2005080846

Hara-Chikuma, M., and A.S. Verkman. 2008a. Aquaporin-3 facilitates epidermal cell migration and proliferation during wound healing. *J. Mol. Med.* 86:221–231. http://dx.doi.org/10.1007/s00109-007-0272-4

Hara-Chikuma, M., and A.S. Verkman. 2008b. Prevention of skin tumorigenesis and impairment of epidermal cell proliferation by targeted aquaporin-3 gene disruption. *Mol. Cell. Biol.* 28:326–332. http://dx.doi.org/10.1128/MCB.01482-07

Jackson, S.H., S. Devadas, J. Kwon, L.A. Pinto, and M.S. Williams. 2004. T cells express a phagocyte-type NADPH oxidase that is activated after T cell receptor stimulation. *Nat. Immunol.* 5:818–827. http://dx.doi.org/10.1038/ni1096

Ludewig, U., and M. Dynowski. 2009. Plant aquaporin selectivity: where transport assays, computer simulations and physiology meet. *Cell. Mol. Life Sci.* 66:3161–3175. http://dx.doi.org/10.1007/s00018-009-0075-6

Ma, T., Y. Song, B. Yang, A. Gillespie, E.J. Carlson, C.J. Epstein, and A.S. Verkman. 2000. Nephrogenic diabetes insipidus in mice lacking aquaporin-3 water channels. *Proc. Natl. Acad. Sci. USA.* 97:4386–4391. http://dx.doi.org/10.1073/pnas.080499597

Martin, S.F. 2004. T lymphocyte-mediated immune responses to chemical haptens and metal ions: implications for allergic and autoimmune disease. *Int. Arch. Allergy Immunol.* 134:186–198. http://dx.doi.org/10.1159/000078765

Miller, E.W., B.C. Dickinson, and C.J. Chang. 2010. Aquaporin-3 mediates hydrogen peroxide uptake to regulate downstream intracellular signaling. *Proc. Natl. Acad. Sci. USA.* 107:15681–15686. http://dx.doi.org/10.1073/pnas.1005776107

Mora, J.R., and U.H. von Andrian. 2006. T-cell homing specificity and plasticity: new concepts and future challenges. *Trends Immunol.* 27:235–243. http://dx.doi.org/10.1016/j.it.2006.03.007

Paulsen, C.E., and K.S. Carroll. 2010. Orchestrating redox signaling networks through regulatory cysteine switches. *ACS Chem. Biol.* 5:47–62. http://dx.doi.org/10.1021/cb900258z

Pittet, M.J., and T.R. Mempel. 2008. Regulation of T-cell migration and effector functions: insights from in vivo imaging studies. *Immunol. Rev.* 221:107–129. http://dx.doi.org/10.1111/j.1600-065X.2008.00584.x

Poole, L.B., and K.J. Nelson. 2008. Discovering mechanisms of signaling-mediated cysteine oxidation. *Curr. Opin. Chem. Biol.* 12:18–24. http://dx.doi.org/10.1016/j.cbpa.2008.01.021

Purushothaman, D., and A. Sarin. 2009. Cytokine-dependent regulation of NADPH oxidase activity and the consequences for activated T cell homeostasis. *J. Exp. Med.* 206:1515–1523. http://dx.doi.org/10.1084/jem.20082851

Reiss, Y., A.E. Proudfoot, C.A. Power, J.J. Campbell, and E.C. Butcher. 2001. CC chemokine receptor (CCR)4 and the CCR10 ligand cutaneous T cell–attracting chemokine (CTACK) in lymphocyte trafficking to inflamed skin. *J. Exp. Med.* 194:1541–1547. http://dx.doi.org/10.1084/jem.194.10.1541

Rhee, S.G. 2006. Cell signaling. H2O2, a necessary evil for cell signaling. *Science.* 312:1882–1883. http://dx.doi.org/10.1126/science.1130481

Rojek, A., J. Praetorius, J. Frøkiaer, S. Nielsen, and R.A. Fenton. 2008. A current view of the mammalian aquaglyceroporins. *Annu. Rev. Physiol.* 70:301–327. http://dx.doi.org/10.1146/annurev.physiol.70.113006.100452

Saadoun, S., M.C. Papadopoulos, M. Hara-Chikuma, and A.S. Verkman. 2005. Impairment of angiogenesis and cell migration by targeted aquaporin-1 gene disruption. *Nature.* 434:786–792. http://dx.doi.org/10.1038/nature03460

Schaerli, P., and B. Moser. 2005. Chemokines: control of primary and memory T-cell traffic. *Immunol. Res.* 31:57–74. http://dx.doi.org/10.1385/IR:31:1:57

Schröder, E., and P. Eaton. 2008. Hydrogen peroxide as an endogenous mediator and exogenous tool in cardiovascular research: issues and considerations. *Curr. Opin. Pharmacol.* 8:153–159. http://dx.doi.org/10.1016/j.coph.2007.12.012

Stone, J.R., and S. Yang. 2006. Hydrogen peroxide: a signaling messenger. *Antioxid. Redox Signal.* 8:243–270. http://dx.doi.org/10.1089/ars.2006.8.243

Takesono, A., R. Horai, M. Mandai, D. Dombroski, and P.L. Schwartzberg. 2004. Requirement for Tec kinases in chemokine-induced migration and activation of Cdc42 and Rac. *Curr. Biol.* 14:917–922. http://dx.doi.org/10.1016/j.cub.2004.04.011

Toda, K., K. Tsujioka, Y. Maruguchi, K. Ishii, Y. Miyachi, K. Kuribayashi, and S. Imamura. 1990. Establishment and characterization of a tumorigenic murine vascular endothelial cell line (F-2). *Cancer Res.* 50:5526–5530.

Tybulewicz, V.L., and R.B. Henderson. 2009. Rho family GTPases and their regulators in lymphocytes. *Nat. Rev. Immunol.* 9:630–644. http://dx.doi.org/10.1038/nri2606

Veal, E.A., A.M. Day, and B.A. Morgan. 2007. Hydrogen peroxide sensing and signaling. *Mol. Cell.* 26:1–14. http://dx.doi.org/10.1016/j.molcel.2007.03.016

Verkman, A.S. 2009. Knock-out models reveal new aquaporin functions. *Handb. Exp. Pharmacol.* 190:359–381. http://dx.doi.org/10.1007/978-3-540-79885-9_18

Viola, A., R.L. Contento, and B. Molon. 2006. T cells and their partners: The chemokine dating agency. *Trends Immunol.* 27:421–427. http://dx.doi.org/10.1016/j.it.2006.07.004

Yang, B., T. Ma, and A.S. Verkman. 2001. Erythrocyte water permeability and renal function in double knockout mice lacking aquaporin-1 and aquaporin-3. *J. Biol. Chem.* 276:624–628. http://dx.doi.org/10.1074/jbc.M008664200

Yang, L., R.M. Froio, T.E. Sciuto, A.M. Dvorak, R. Alon, and F.W. Luscinskas. 2005. ICAM-1 regulates neutrophil adhesion and transcellular migration of TNF-alpha-activated vascular endothelium under flow. *Blood.* 106:584–592. http://dx.doi.org/10.1182/blood-2004-12-4942

Yoo, S.K., T.W. Starnes, Q. Deng, and A. Huttenlocher. 2011. Lyn is a redox sensor that mediates leukocyte wound attraction in vivo. *Nature.* 480:109–112. http://dx.doi.org/10.1038/nature10632